PROCEEDINGS, 50th Workshop on Geothermal Reservoir Engineering
Stanford University, Stanford, California, February 10-12, 2025
SGP-TR-229

Tracer Return Analysis in Volsung using Particle Tracking

Peter Franz[1], Jonathon Clearwater[1], Tim Mitchell[1], Ethan Chabora[2]

[1]Seequent, 20 Moorhouse Avenue, Addington, Christchurch 8011, NEW ZEALAND

[2]Contact Energy Ltd, Private Bag 2001, Taupo 3352, New Zealand

Peter.Franz@seequent.com

Keywords: Volsung, Tracer, Geothermal, Modelling.

ABSTRACT

Injection tracers are an important tool for geothermal reservoir engineers to monitor fluid return from injection to production wells and understand reservoir flow paths. Fast return times indicate a direct connection between injection and production sites, and field development strategies are modified to mitigate thermal breakthrough between the wells. Tracer data can also be very helpful in calibrating numerical models to provide greater confidence in model forecasts. Traditionally, tracers have been modelled as an additional mass component in the control volume method. However, this is problematic due to the discretized nature of reservoir models. Reservoir models often use grid blocks with greater than 100 m scale grid blocks and, when modelling tracers as additional mass components, numerical dispersion can strongly influence tracer simulation results. Numerical dispersion tends to smear out the tracer return; however, numerical dispersion will be dependent on grid block size, and it is not the same as actual hydrodynamic dispersion. Furthermore, modelling tracers as an additional mass component significantly increases simulation run times. Streamline modelling treats the tracer problem differently. In our work we model the tracer as an ensemble of virtual tracer particles which move through the reservoir along the velocity field established by the reservoir simulator. This allows the tracer to move as a sharply defined front, with the return curve shape reflecting different pathways through the reservoir and their relative importance. In this paper we describe the tracer particle methodology, present some validation models for the streamline approach, and compare the new approach with results from the control volume method.

1. INTRODUCTION

1.1 Introduction to tracers and their value for managing geothermal resources

A tracer is a chemical that is injected into a well and measured at a production well. The chemical may be an artificial tracer that is injected as a pulse into a selected well during a dedicated tracer test, or a natural tracer, such as chloride. Tracer tests are widely used in the geothermal industry. The tracer data can be analyzed to give a deeper understanding about reservoir flow paths, and since chemical breakthrough occurs much faster than thermal breakthrough, they can provide an early warning on the risk of enthalpy decline. Tracer data can also be simulated directly with a numerical model and used to calibrate the model to give a greater confidence in model predictions.

Tracers provide quantitative data that can be analyzed to aid in the understanding of reservoir connectivity and the characterization of reservoir flow-paths. This supports the sustainable, cost-effective development of geothermal systems by enabling better reservoir management and giving greater confidence in predictions of future reservoir behavior. Reservoir management includes both production and reinjection strategies, and optimizes reservoir performance while decreasing risk, minimizing costs and mitigating negative environmental impacts. A typical reinjection strategy seeks to reinject fluid back into the geothermal system to support reservoir pressure and well production, while minimizing enthalpy decline. If injection wells are located too close to production wells, or on reservoir flow paths with a direct connection to production wells, then there is a risk that the cooler injected fluid will short-circuit and flow directly to the production wells causing premature cooling. If the injection wells are targeted too far away from the production wells, or in areas without any permeable connection to the production zones, then the reinjected fluid may not provide sufficient pressure support and well production may decline rapidly. A better understanding of reservoir flow paths via tracer data analysis enables better reservoir management, and because this impacts production flow rates, decline rates and enthalpy, it has a significant impact on overall project costs (drilling) and revenue (generation).

1.2 Introduction to Volsung

Volsung is an integrated simulation platform designed for the geothermal industry with a rapidly growing user-base (Clearwater et al. 2024). It includes a reservoir model that simulates multi-phase, multi-component flow of heat and mass through porous and fractured media, a wellbore model to account for the flow of fluid from reservoir feed zones to wellhead, and a surface network simulator to model fluid movement through surface pipeline networks, separators and power plants (Franz et al. (2019), Clearwater and Franz (2019), Cinco et al. (2020), Franz and Clearwater (2021), McLean et al. (2020), Baxter et al. (2023)).

1.3 Theory of Tracer Flow

Tracers are chemicals that are dissolved in the reservoir fluid and they flow according to three principal transport modes:

1. Advection – transport of tracer via convective reservoir fluid flow.
2. Mechanical dispersion – spreading out due to local differences in fluid velocity and heterogeneity. Described as longitudinal when the spreading is in the same direction as the main reservoir fluid velocity or transverse when it is perpendicular to the main flow.
3. Molecular diffusion – the movement of tracer along chemical concentration gradients.

The term hydrodynamic dispersion refers to the combined process of mechanical dispersion and molecular diffusion. The dominant process in most geothermal solute transport is advection, as it is the flow of reservoir fluid that dominates the movement of the tracer throughout the reservoir. Mechanical dispersion is also important, and we often see a characteristic lag between the first arrival time of a tracer and the peak along with "long tails", indicating dispersion of the tracer as it flows from injector to producer. A synthetic example of tracer data is shown in Figure 1 with a first arrival time of 45 days, a peak arrival of 140 days and a slightly longer tail of tracer data extending out to 400 days. In most geothermal applications we can ignore molecular diffusion as it is a relatively slow process in comparison to advection, however this should be considered on a case-by-case basis.

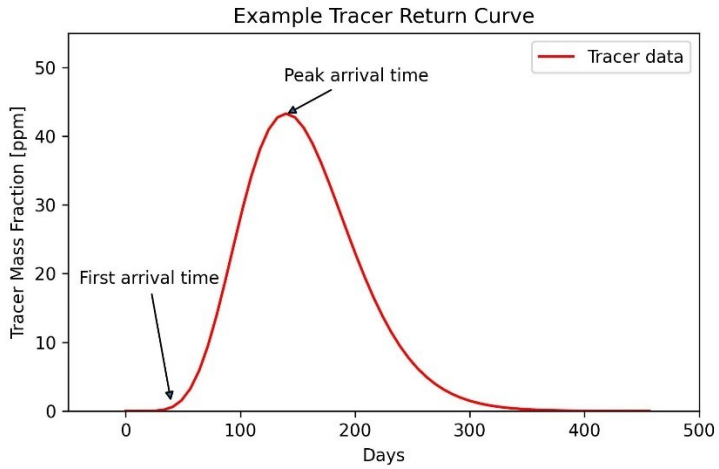

Figure 1: Synthetic example of a tracer return curve showing the first arrival time, peak arrival time and the shape of the curve.

1.2. Analyzing tracer data

There are several approaches to analyzing tracer data. The simplest is just plotting the data and comparing first arrival times, peak arrival times and the shape of the return curves for different wells. This basic approach yields a qualitative assessment of reservoir connectivity indicating production and injection wells that have either strong or weak connections and provides valuable information with which to update the conceptual understanding of the reservoir. Another approach is to analyze the data quantitatively to calculate the mean residence time, swept pore volume and flow geometry using the temporal moment analysis (Shook and Forsmann, 2005) or match the tracer data with simplified models to characterize the flow paths and make predictions of future cooling trends (Axelsson, 2005). The approach we address in this paper is to analyze the tracer data by using a numerical reservoir simulation model. Most operating geothermal fields have a reservoir simulation model. These models are typically based on an integrated geoscientific understanding of the resource, calibrated to field data and used for predicting future field behavior and managing the resource. In an ideal world we would simply add the tracer test into the numerical model and match the model to the tracer data as a calibration process. This would quantitatively test our understanding of reservoir connectivity, improve the numerical model and foster greater confidence in model predictions. In the real world, however, this is only done in a small subset of cases due to the challenges of simulating tracer tests with numerical simulators, and it is these challenges that we are attempting to overcome by adding particle tracking into Volsung.

1.3. Simulating tracer tests with numerical models

Commonly used geothermal reservoir simulators, such as TOUGH2 (Pruess, 1999), Waiwera (Croucher, 2018) and Volsung (Franz and Clearwater, 2019), use finite volume numerical methods to solve the multi-phase and multi-component mass and energy balance equations. In these simulators, tracers can be modelled as an additional mass component. However, this approach is problematic for two reasons. First, treating the tracer as an extra component slows down simulation times. The additional component increases the size and complexity of the linear system, thus slowing down the iterative solver used to satisfy the heat and mass balance equations. Treating the tracer as an additional component also changes the primary variables used by a simulator to define the properties of the fluid in the model, so it is common for users to need to rerun models to natural state conditions with a different equation of state that includes the tracer, before simulating the specific tracer test. Since the small amounts of tracer do not normally change the fluid properties, treating the tracer as a new and independent component is unnecessary and leads to needless delays in the modelling process. The issue of slow model run times with tracers can be partially addressed with modern simulators that run in parallel and reduce simulation times by about an order of magnitude compared to traditional single threaded simulators. Another approach is to treat the tracers as passive components in the system

and solve the tracer flow equations separately from the flow equations (Croucher et al. 2021; Burnell et al. 2021). The second issue, when modelling tracers as additional mass components, is that the results can be highly dependent on the grid size and orientation due to numerical effects. This issue is trickier to overcome. In a numerical scheme the subsurface is split in discrete regions of space known as grid blocks, and the solution is solved forward in time for discrete timesteps. Numerical approaches with time and space discretization do not solve partial differential equations exactly, they always introduce some type of error, so any simulation model will have different characteristics to the real physical process being modeled. In practice, in most applications of geothermal reservoir models we can keep any concerns about numerical effects safely in the back of our minds as the impact on confidence in model predictions is minor. When it comes to modelling tracers using reservoir models, however, these numerical effects have a very significant impact on model behavior. An illustration of this is shown in Figure 2 demonstrating how the tracer concentration can spread out due to numerical dispersion.

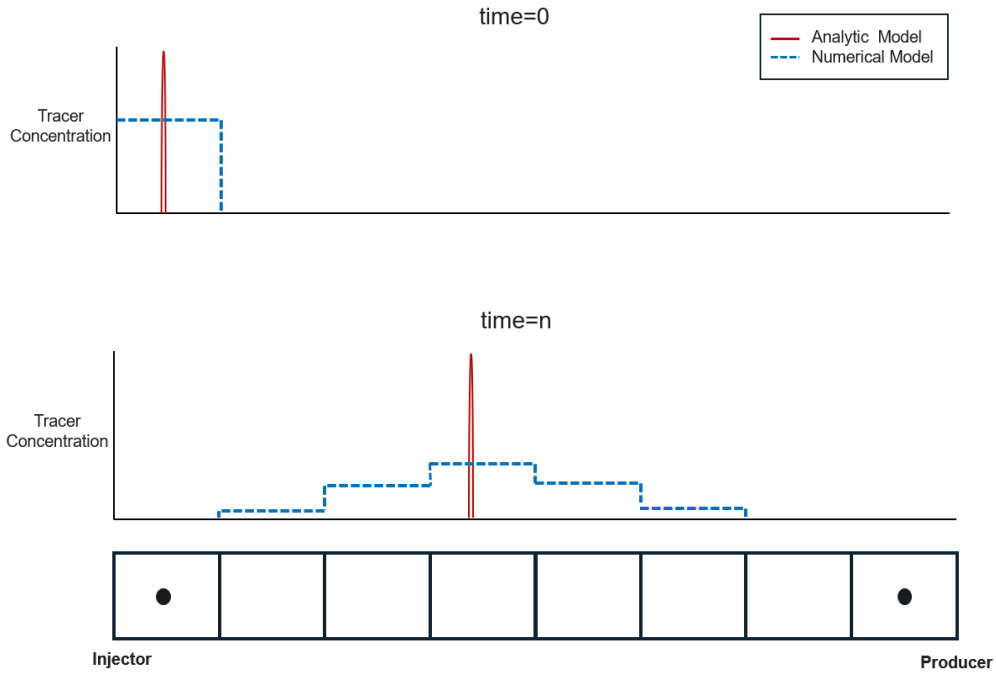

Figure 2: An illustration showing the propagation of a pulse of tracer moving from an injection well on the left to a production well on the right. The red curve shows the theoretical propagation and the blue dashed line represents how this could spread during propagation in a simulation model due to numerical dispersion.

Care must be taken when discussing dispersion in the real world and in simulation models. Hydrodynamic dispersion is a spreading process that occurs in the real world whereas numerical dispersion is a spreading out process that occurs in numerical models that is dependent on grid block size and the numerical methods used. Numerical dispersion is not the same as actual hydrodynamic dispersion and relying on numerical dispersion to model hydrodynamic dispersion can lead to poorly calibrated models. There have been several attempts to overcome the issue of numerical dispersion in geothermal simulation codes, including trying higher order total variation diminishing schemes (Oldenburg and Pruess (1997), Oldenburg and Pruess (2000), Wu and Forsyth (2006)) or converting models to use Eulerian–Lagrangian methods in a finite element context (Croucher et al. 2004), but most have led to slower run times and have not achieved widespread use within the industry.

In Volsung we have implemented an alternative method known as particle tracking. In this approach, the finite volume method is used to solve the flow equations and approximate a velocity field in the model, and then tracer particles are assumed to move along these velocity field lines. A similar method is implemented in ModFlow for groundwater modelling applications (Pollock, 2012). The tracer particle method has several advantages over the additional component method:

1. Particles can be located at any point in space – they are not restricted to be located at block centers. Because of this we can model how each particle will travel through a grid block, whereas in the additional component method, we only model the concentration of the tracer mass fraction over a grid block volume.
2. Solving the flow equations for the tracer particles is fast and independent of the underlying heat and mass flow equations in the reservoir simulator, so it does not cause a significant slowdown in simulation run times.
3. The tracer particle method does not change the underlying equation of state, so the user does not need to manage primary variables and initial conditions.

2. METHODOLOGY

2.1. General Approach

Tracer particles are handled as an "Extra Module" in Volsung. This means that calculations are performed after the flow solution of the reservoir simulator has been established for a given reservoir simulation time step.

The velocity field is approximated using the calculated flow solution. Tracer particles are injected into this velocity field on random points on a sphere around an injection feed zone and start to move along the velocity field lines using a simple Euler step transport scheme. Transport timesteps are specific for each particle, and they are adapted using the dimensions of the block in which the particle is currently located. The intention is that each particle should sample the block it resides in approximately five times. This is important when dealing with tracers which exhibit thermal breakdown and prevents the tracer particle leaving a block too soon due to the discretized movement (overshooting). This timestep for the tracer particle movement is also independent of the timestep for the finite volume flow solution, so it is possible, for example, to have the overall reservoir simulation take timesteps of several weeks while the tracer particles are iterated hourly to allow the particles to follow a more convoluted pathway.

A tracer particle can be absorbed by a reservoir sink in two ways. If the sink is a general sink (i.e. it is thought to absorb fluid from the whole block), then the tracer particle is absorbed using a probabilistic approach, using the sink rate and present mass of fluid to determine the absorption probability. The second way of getting absorbed is by entering a set absorption sphere around a production feed zone. Absorbed particles track their absorption time and the sink identifier, enabling the calculation of tracer breakthrough analysis for each tracer at each sink.

2.2. Phase Changes

Some tracers preferentially partition into either the vapor or liquid phase. At the beginning of each timestep, the tracer particle can change the phase of fluid in which it is transported. The phase partitioning probability takes the current phase mass fractions and possible phase fractionation into account. It is possible that a tracer prefers to be in a specific phase and this is set by giving that phase a higher phase partitioning constant.

2.3. Decay

During each timestep a tracer can experience thermal breakdown or radioactive decay; this is achieved by reducing the mass of the tracer particle accordingly, either by exponential decay using a half-life constant for radioactive tracers, or by Arrhenius-style thermal breakdown using a pre-exponential factor and activation energy (Arrhenius, 1889).

2.4. MINC

If a block contains Multiple Interacting Continuum (MINC) (Pruess and Narasimhan, 1985) layers then the particle only gets transported while it is in the outermost (fracture) layer. At each timestep the particle has the possibility to be either absorbed into or released from an adjacent MINC layer. The transition probabilities are calculated from the fluid transport rates into or out of the adjacent MINC layers, and the amount of fluid present in the current residing layer. It is hence possible for a particle to get locked into place by being absorbed by a MINC layer and being released later so it can continue its journey through the reservoir.

2.5. Velocity Field

The solution to the finite volume flow simulation gives the fluid velocity at the connections between each cell in the model. In the particle tracking method, a particle could be located anywhere in space, so a velocity field needs to be calculated. Volsung provides two methods for calculating the velocity field. The first option is to use a least-squares linear approximation to the flux vectors at the centers of the cell faces. A Moore-Penrose pseudo-inverse matrix is used to calculate the velocity field inside a cell. The second option for calculating the velocity field is with the flux interpolation method described in Klausen et al. (2012) section 4 known as mimetic finite difference (MFD) interpolation. With this approach, a velocity field that exactly interpolates the flux across the cell faces is constructed.

These two methods give the same results on axis aligned structured or tartan grids; however, the second method gives more accurate results for unstructured grids. This is illustrated in Figure 3 below.

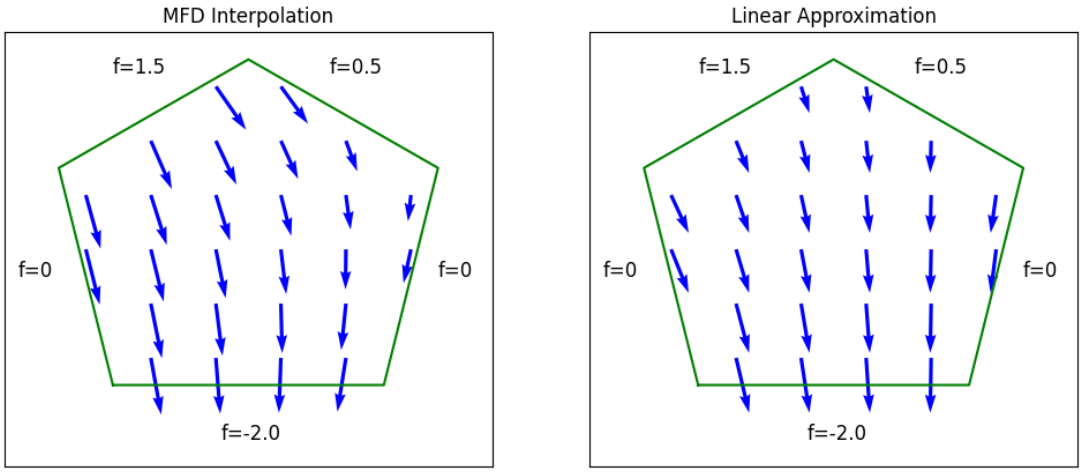

Figure 3: A synthetic example showing the difference in the two velocity interpolation options for a pentagonal cell. The fluxes for each edge are shown with an overall flow of 2 units downwards. The left side shows that the MFD interpolation reproduces the difference in flux across the top two faces and the no-flow side faces. The right side shows the Linear approximation that has averaged the flow across the top two faces and the no-flow side faces.

3. VALIDATION

3.1. Horizontal 1D Model – liquid

We created a one-dimensional, horizontal flow model 1100 m in the x-direction and 100 m x 100 m in the y and z directions. This model was split into 11 100 m x 100 m x 100 m grid blocks. An injection well was placed in the first grid block and a production well was placed in the last grid block so that they were spaced 1000 m apart. The model had a uniform porosity of 10% and permeability of 1000 mD in all directions. The initial conditions for the model were set at 10 bar and 420 kJ/kg. The model was run in Volsung with a constant production rate of 20 kg/s and constant injection of pure water at 20 kg/s at 420 kJ/kg. This allowed the model to generate a stable pressure gradient across the model with about 13 bar in the injection grid block and 7 bar in the production grid block. These stable conditions formed the initial conditions for tracer simulations, which were simulated by both the particle tracking method and the two-component finite volume method.

Since this is a simple steady state, 1D flow model the tracer arrival time can be calculated analytically. Fluid velocity v in this scenario is

$$v = \frac{w}{A\rho\varphi}$$

where w is the steady-state mass flow between producer and injector, A is the cross-sectional area of the vertical faces of the blocks, ρ is the fluid density and φ is the porosity. This gives a fluid velocity of 20.9 μm/s and an expected tracer arrival time of 555 days (~1.5 years).

Traditionally geothermal tracer tests have been simulated as an additional mass component in the control volume method. To compare the new particle tracking method to the traditional approach we created a set of simple models and compared the tracer returns between the new Volsung Tracer Particle method and traditional methods using Volsung and TOUGH2. Since numerical dispersion depends on grid size, we repeated the same study with 10 m grid blocks in the x-direction. Results from this model are shown in Figure 4 and Figure 5.

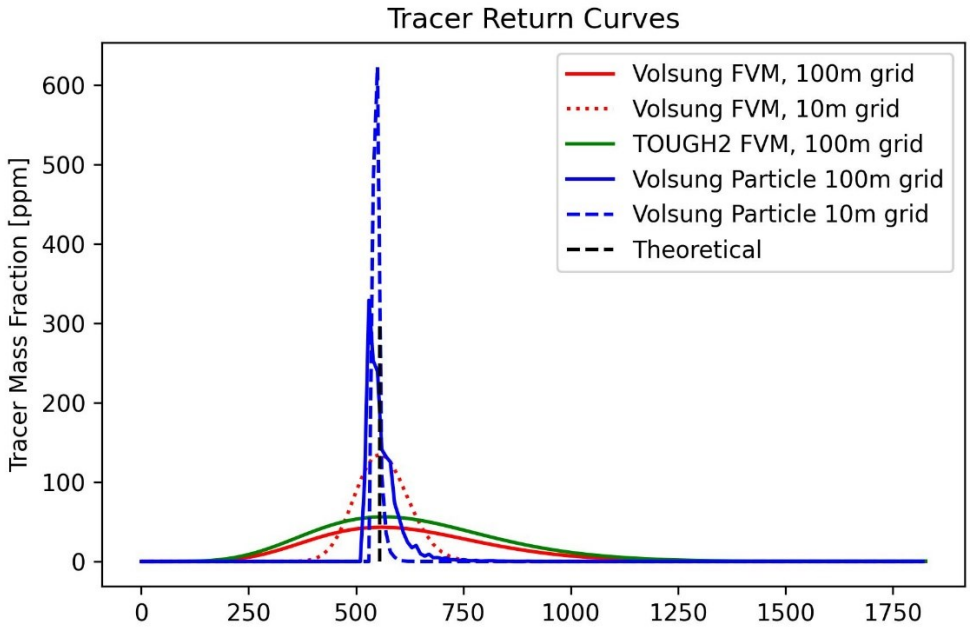

Figure 4: Results from the 1D horizontal model in liquid conditions. The black dashed line shows the 555-day expected arrival time that was calculated analytically. The blue solid line shows the tracer particle method with 100 m grid spacing and the blue dashed line shows the particle method with 10 m grid spacing. The other results are all from the 2-component finite volume method using either 100 m or 10 m grid run with either Volsung or TOUGH2, as indicated in the legend.

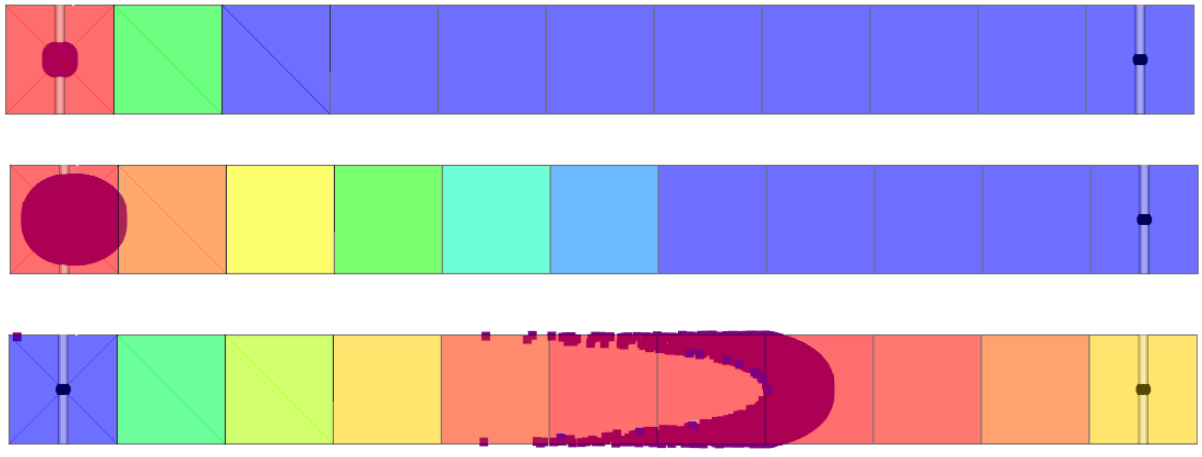

Figure 5: A slice through the 1D horizontal model showing the tracer particles with model grid blocks colored by tracer concentration. The color is on a log scale with blue indicating an undetectable amount of tracer (<1 ppb) and red indicating 100 ppm. The injection well is on the left and the producer is on the right. The top plot shows the state of the model one day after tracer injection, the middle plot is 15 days after tracer injection and the bottom image is about 1 year after tracer injection.

These results for the additional component finite volume method show that for a 100 m grid model, in both Volsung and TOUGH2, the first arrival time was about 240 days and the peak arrival time of about 550 days. The peak arrival time corresponds well with the theoretical arrival time, but the first arrival time was about 300 days early. When the grid size was reduced to 10 m the first arrival time was about 400 days and the peak arrival time was unchanged. In these simulations there was not an explicit model for mechanical dispersion or molecular diffusion, so all of the dispersion was due to numerical effects, and we can see the dependency of grid size with the change in first arrival time from 240 to 400 days with the change in grid block size. The first arrival time did not agree with the

expected arrival time calculated theoretically and was strongly influenced by numerical effects and grid block size. The peak arrival time was in good agreement with the expected arrival time.

The results for the tracer particle method show a sharp first arrival front with a first arrival time of 526 for the 100 m grid block model and 547 days in the 10 m grid block model. The tracer results were binned into 10-day histograms for analysis and the peak arrival time in the 100 m grid block model was in the 530-540 day bin and the peak arrival time in the 10 m grid block model was in the 540-550 day bin, these are both slightly earlier than the 555 day theoretical arrival time. The particle tracking method gave closer results to the theoretical arrival times and did not have as much dispersion as the additional component finite volume method. It did, however, still have some dispersion, and this occurred in a model where we did include an explicit model for hydrodynamic dispersion. The reason the particles were spread out was because of the method used of originally placing the particles randomly on a sphere around the injection well and adding the $1/r^2$ velocity term in the source/sink blocks gives the potential for particles to move faster and at more variable velocities in the source and sink blocks.

3.1. Horizontal 1D Model – 2-phase

To validate the tracer simulation in 2-phase conditions we created a simple one-dimensional, horizontal flow model, consisting of 21 blocks of dimensions 100 m x 100 m x 100 m. An injection well was placed in the center of the first block, and a producing well in the center of the last block, i.e. they are spaced 2000 m apart. The porosity was set at 10%. The initial conditions in the reservoir were a uniform 56 bar and an enthalpy of 1200 kJ/kg, which gives 2-phase conditions with a gas saturation of 13.4%. Production was set at 20 kg/s and the injection well injected 20 kg/s fluid at 1200 kJ/kg; this value was chosen to match the enthalpy of the initial conditions in the reservoir. The permeability was set at 10 Darcy to minimize the pressure gradient between the injector and producer. For the relative permeability, linear X-crossover functions were implemented so that the relative permeability equals the saturation for both liquid and gas phases. The model was run for one million years and stabilized to steady state flow. Under stable flowing conditions the average gas saturation in the model was about 14.9% and the pressure about 49.3 bar. Under these 2-phase conditions the phase velocity for phase β can be calculated by

$$v_\beta = \frac{w}{A}\frac{f_\beta}{\rho_\beta \varphi S_\beta}$$

where f_β is the flowing fraction of the phase and S_β is the phase saturation. f_β can be calculated from the ratio of the phase mobility to the total mobility, with mobility defined as the phase relative permeability multiplied by the phase density and divided by phase viscosity.

Using thermodynamic values for the initial state of the simulation we calculated values for the liquid and gas velocity to be around 29.3 and 166 μm/s, respectively. Calculated peak arrival times for the liquid and gas phases are 790 and 139 days, respectively.

We ran this model with three different tracer behaviors; the base model uses equal-phase partitioning of the tracer. In the other two models, the tracer was allowed to only flow in either the liquid or the gas phase.

Figure 6 shows the tracer breakthrough curves at the producing well. The single-phase models have tracer arrival at 762 days and 139 days for the liquid and gas phase, respectively. The gas phase model hence agrees very well with the manually calculated arrival times. The liquid phase model shows slightly faster arrival times; however, it needs to be kept in mind that the fluid travels faster in the source/sink blocks due to the $1/r^2$ velocity due to the source/sink terms. If travel time in these blocks was considered negligible, this would reduce the travel time to ~751 days. The modelled arrival time of 762 days hence falls into the bracketing solution of 751 to 790 days.

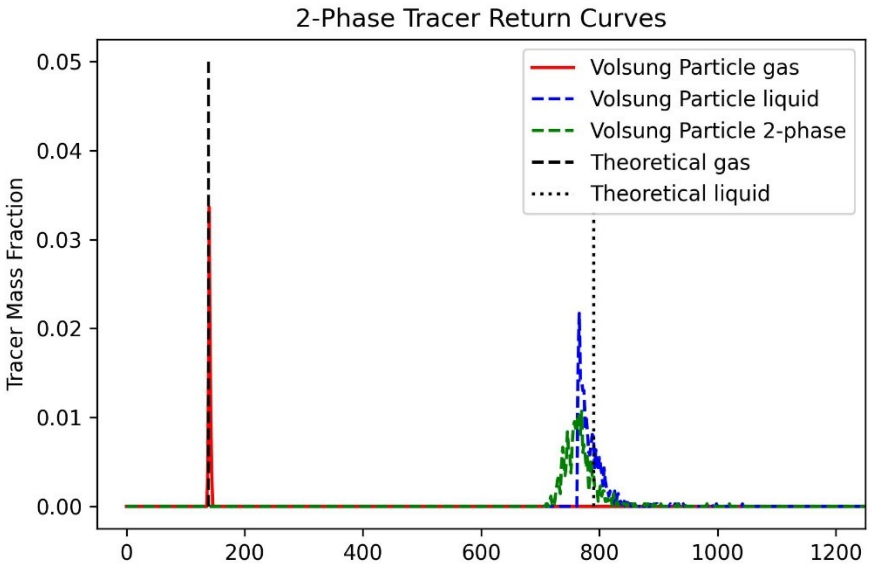

Figure 6: Tracer return curves for a 1D horizontal model with 2-phase reservoir conditions.

The base model, where tracer particles can move in both phases, has first tracer arrival at 702 days and peak arrival at 751 days. These results can be explained by the fact that most transport by mass – approximately 99.4% – is in the liquid phase. The 0.6% of tracer flowing in the faster gas phase gets repeatedly reabsorbed into the liquid phase at each time step for the tracer particle simulation. A small number of tracer particles can hence travel faster in the gas phase for a little while, but then get reabsorbed into the liquid phase and travel slower again. The result is a broadening of the tracer breakthrough curve, but it is still dominated by the liquid phase velocity. This behavior is consistent with our understanding of tracer transport.

4. APPLICATION TO TRACER TEST DESIGN USING AN EXISTING RESERVOIR MODEL

To further explore the practical applications of the tracer particle methodology, a series of hypothetical tracer simulations – using both particles and additional aqueous components – were conducted using an existing numerical model of a commercially active geothermal system. Although this model was previously developed in Volsung for different objectives, it contains sufficient complexity and is reasonably calibrated to historical field data to make it an adequate representation of a real-world case. While many of the technical details of the numerical model will not be discussed here, the basic grid geometry is summarized in Table 1.

Table 1. Basic Grid Properties of the Numerical Model

3D Grid Extent	18 km x 12 km x 4 km
Representative Grid Block Size	400 m x 300 m x 250 m
Grid Block Count	18,816

Four distinct, non-reactive tracers were assigned to unique injection wells in different regions of the model. At each location, both particle and aqueous component tracers were injected into the target well at equivalent rates and concentrations. A 10-year forecast scenario was then simulated by extending the last historical production and injection rates of the active wells in the model. The simulated distribution of the particle and aqueous component tracers were first compared spatially at selected time intervals and then further analyzed using conventional tracer return plots.

The four panels in Figure 7 show the distribution of the tracer particles throughout the grid at different time steps during the simulation. After one month of injection (panel A), the particles are highly concentrated within a tight radius around the injection wells (all of which have multiple feed zones across a range of elevations in the model). Throughout the simulation (panels B-D), the particle swarms become more distorted and variably distributed throughout the grid as distinct flow paths – influenced by geospatial heterogeneity and the flow fields of active wells – are revealed. It should be noted that the tracer particle population in the grid is reduced each time a particle is "captured" by a producing well. This is most apparent in the case of the particles injected at location INJ 3, which is adjacent to two active production areas.

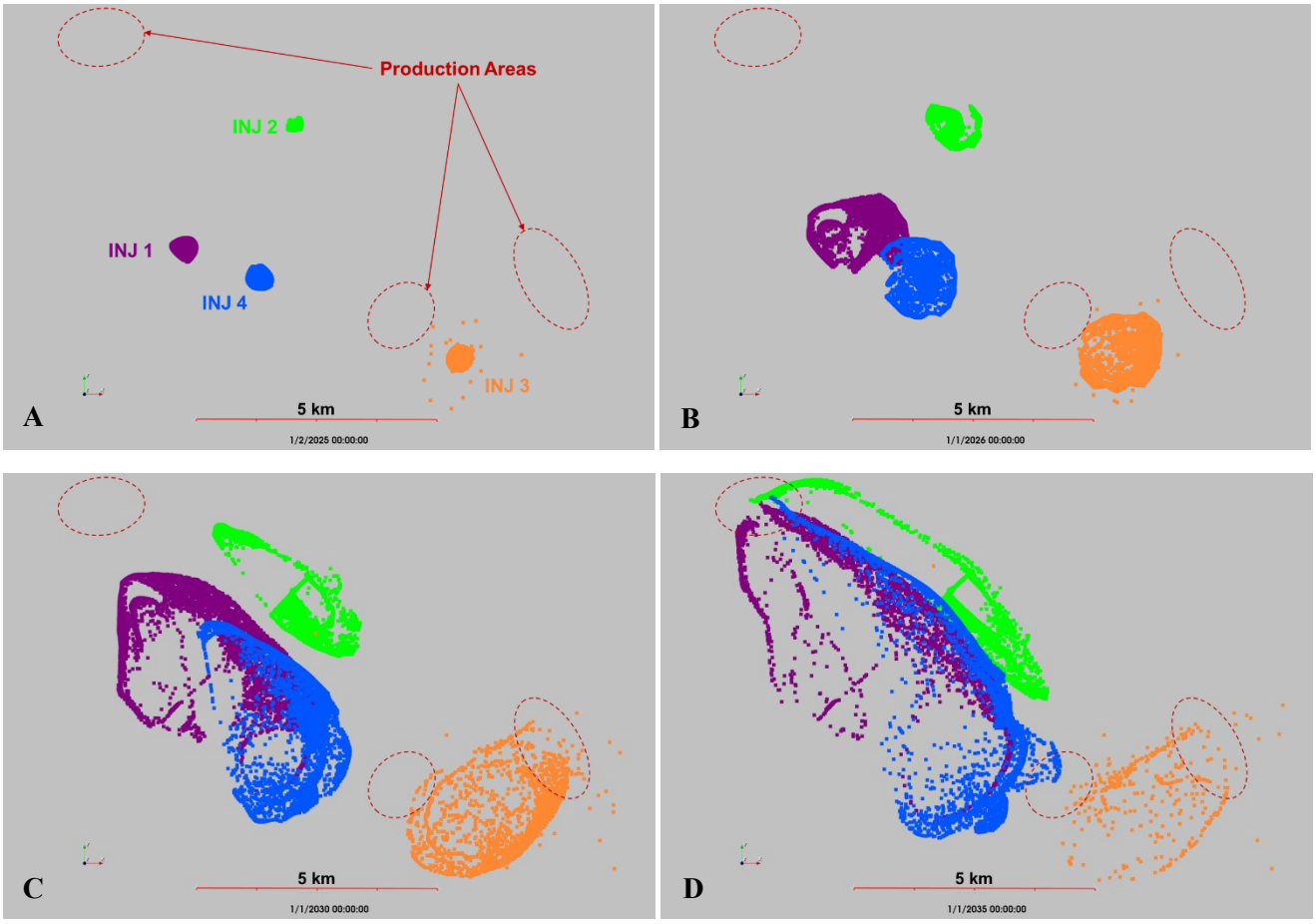

Figure 7: Map view of the simulated particle tracer distributions at different time steps after injection: A) 1 month, B) 1 year, C) 5 years, and D) 10 years.

A comparison of the aqueous component tracer distribution to that of the particle tracer for injection location INJ 4 at four different simulated time steps is shown in Figure 8. The effects of numerical dispersion inherent to the finite volume method are immediately apparent after a quick inspection, particularly after 1 and 5 years of simulated time (panels B and C). At these time steps, the footprint of the grid blocks with aqueous tracer (above the nominal background) is substantially larger than the silhouetted area of the tracer particles. The long axis of the respective distributions in panel C, for example, differs by a factor of approximately 2. After 10 years, the difference in longitudinal extent is less pronounced since both the particles and the aqueous components have reached the main production area in the northwest by this point. Nonetheless, the areal as well as the volumetric extents of the aqueous tracer are still significantly larger compared to those of the particle tracer.

Another salient observation from Figure 8 is that the pattern of aqueous tracer concentration is generally consistent with the spatial density of particles at each time step. This is most noticeable in the 5- and 10-year time steps (panels C and D in Figure 8) where the color shading of the grid blocks can be seen to vary with both the shape and clustering of the underlying tracer particles. Note that the outer grid blocks show very low aqueous tracer concentrations as these areas reflect the leading edge of the numerical dispersion effects. Figure 9 shows that this behavior is preserved vertically through the reservoir as well. In this case of INJ 4, the injection well has three feed zones in three separate grid layers – the shallowest being the most prolific – which distribute the tracers in a disproportional way across the reservoir. Tracer concentration shading of the grid blocks across layers can also be seen to correspond to the tracer particle location and density which varies through time accordingly (compare panels A and B).

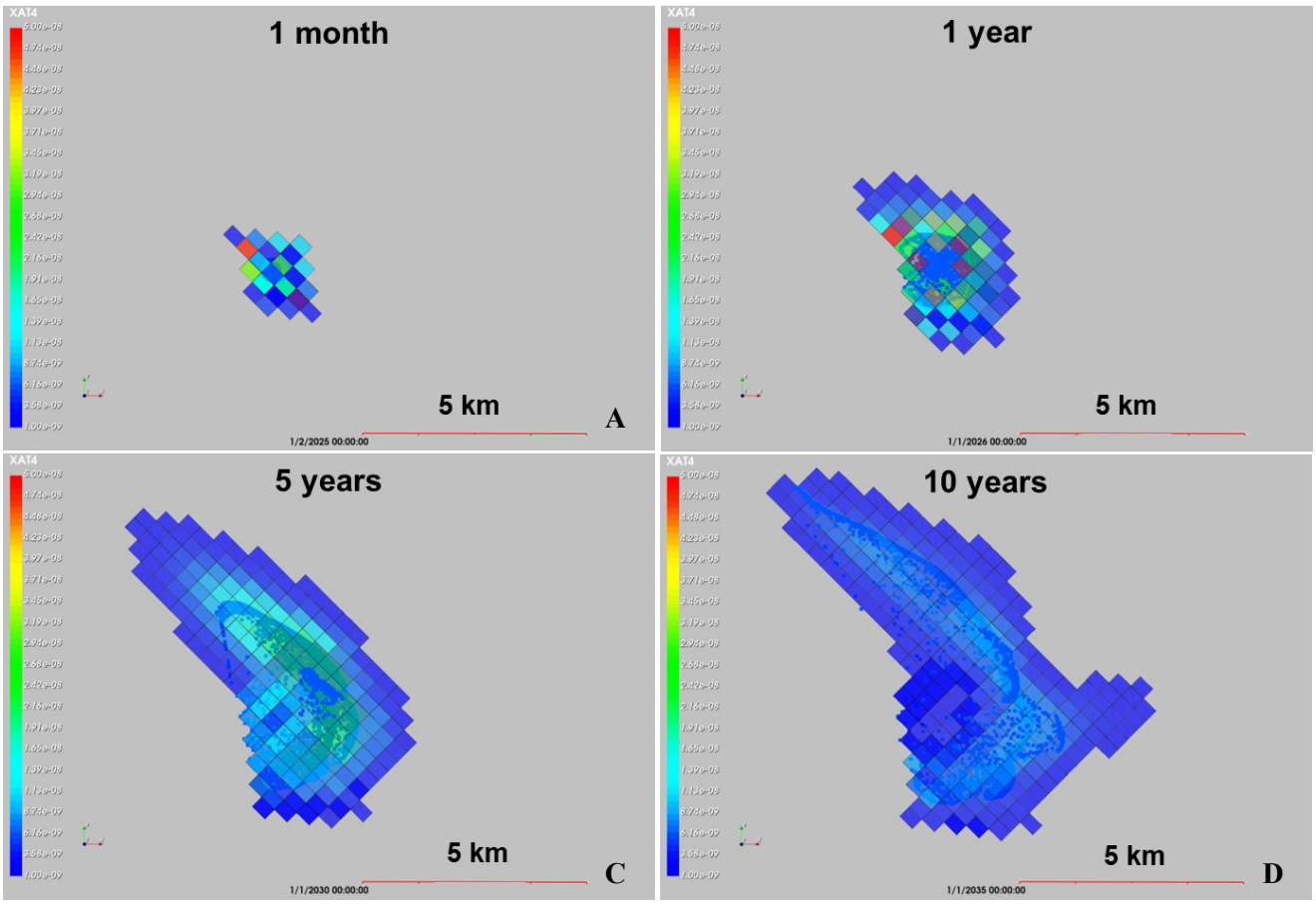

Figure 8: Map view of the simulated aqueous component tracer distribution for INJ 4 compared to that of the particle tracer at different times after injection: A) 1 month, B) 1 year, C) 5 years, and D) 10 years.

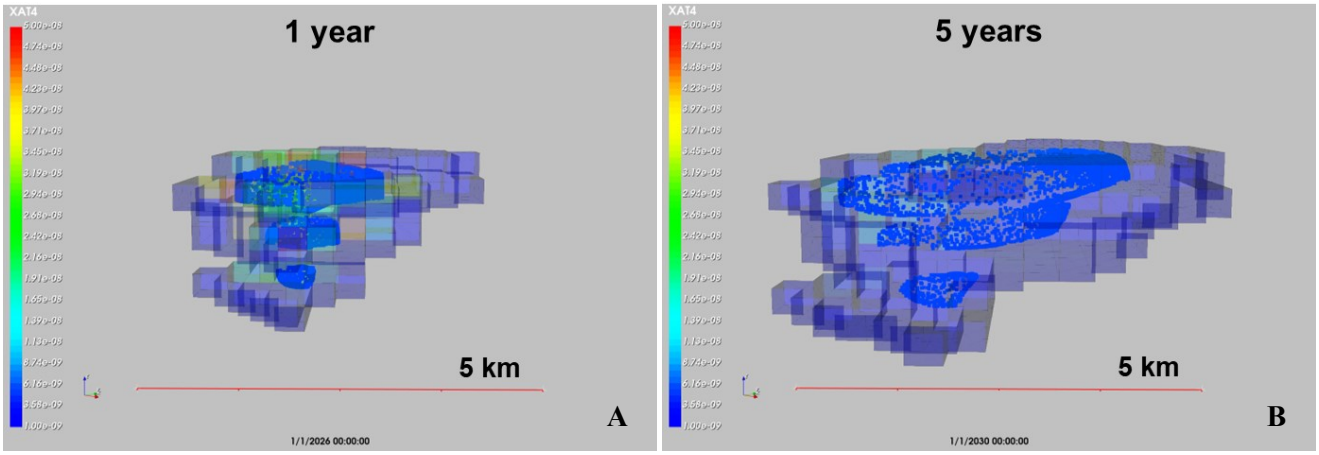

Figure 9: Oblique 3D view of the simulated aqueous component tracer distribution for INJ 4 compared to that of the particle tracer at different times after injection: A) 1 year and B) 5 years.

A more direct, quantitative comparison of the responses is depicted in the tracer return plots shown in Figure 10. To construct each plot, the production wells with the highest mass recovery of each of the four particle tracers were used as the references to compare the corresponding aqueous tracer returns. This approach ensured that there would be sufficient recovery statistics to enable a meaningful comparison between the tracer methods.

One initial observation from the tracer return plots in Figure 10, is that Tracers #1, #2 and #3 show similar characteristics, with the aqueous component and particle methods having a similar peak arrival time, while Tracer #4 exhibits a difference in character between the aqueous component response and the particle tracer response. Tracer #4 shows a bimodal distribution in the particle repsonse with the later peak being larger than the earlier peak. This tracer particle response can be explained in part by referring back to Figure 9, which shows the

vertical migration of particles across layers towards a production well with two feed zones that are shallower than the injection feed zones at INJ 4. It is the arrival of particles at this shallower feed zone that results in a second "wave" of returns later in time. In contrast, the aqueous component tracer shows a smooth unimodal response with no indication of a later peak. This conspicuous difference suggests that the finite volume method is masking the response of multiple flow paths with different transit times that are present in the particle tracer response.

Other important distinctions in the responses include the discrepancy in first arrival and peak arrival times. In each case, the first arrival of the aqueous component tracers is significantly earlier than that of the particle tracers, ranging from ~500 to ~1,300 days earlier. With respect to the peak arrival, there is more variability and each case appears to be slightly different. For Tracers #3 and #4, the aqueous component peak is slightly delayed (~250 days) compared to the initial peak of the particles. For Tracer #1, the aqueous component peak is noticeably early (~400 days) compared to the true peak of the particles. Finally, in the case of Tracer #2, it is not possible to see the full expression of either the aqueous component or particle tracer response due to the duration of the simulation. It does appear visually, however, that the Tracer #2 peak arrivals may be closer in time compared to the other examples, potentially due to a more uniform, slower pathway (as indicated by the later first arrival time). While the peak arrival time for the two tracer methods was similar in the simple, homogeneous system (e.g., Figures 4 and 5), it is noteworthy to observe this range of disparity in a heterogeneous, real-world example.

Another feature of the tracer return plots in Figure 10 is the difference in peak concentration for each method. In each case, the peak particle concentration is higher than that of the aqueous component tracers. This is explained by the discrete nature of the particles, which represent "mass packets" of tracer that remain intact as they traverse their streamline pathways through the grid. The aqueous component tracers, on the other hand, grow more diffuse with each time step due to numerical dispersion, resulting in the same total mass of tracer (in this example) distributed throughout a much larger volume and, therefore, lower concentrations observed upon "capture".

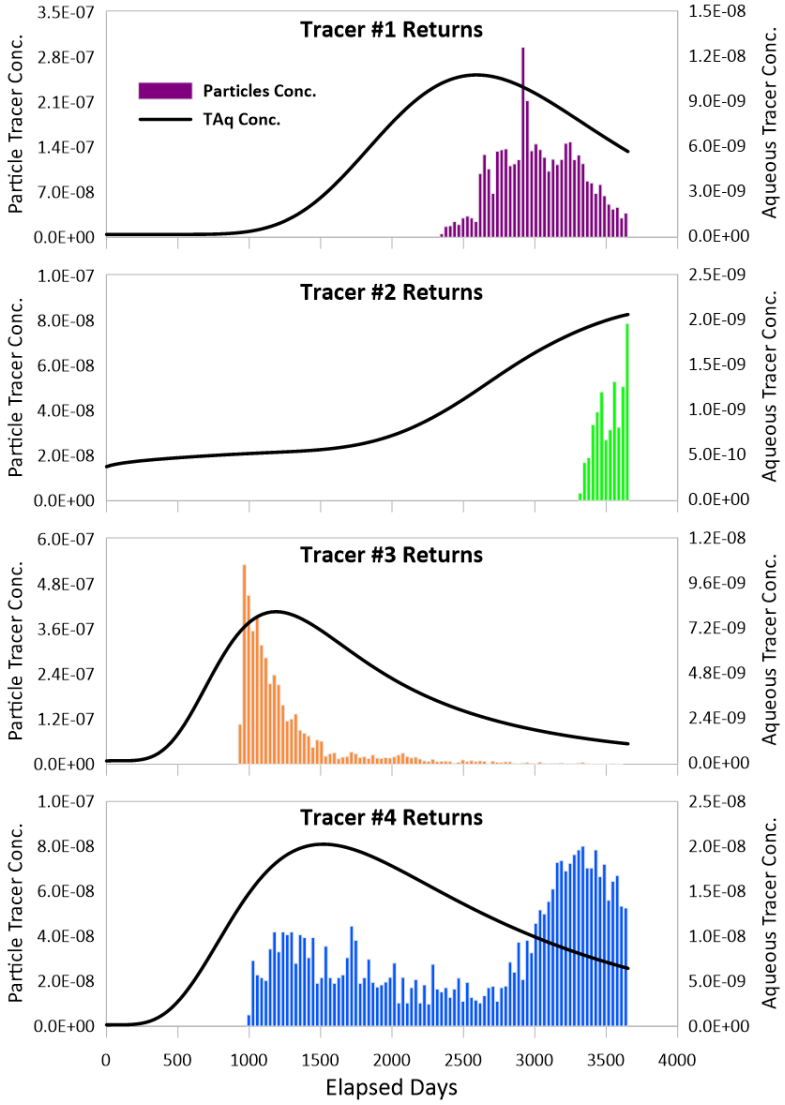

Figure 10: Tracer return plots comparing tracer particles (in colored bars) to aqueous tracer (Taq) components (black lines) from each of the four injection areas. Particle return historgrams are aggregated in 30-day bins.

As illustrated by the previous example, the particle tracer methodology creates a portrayal of the predicted tracer behavior in an active geothermal system that has both similarities and differences compared to the conventional aqueous component approach. This alternative view has potential bearing on the design, execution, and interpretation of the results from field tracer tests. For example, the variability of the simulated first arrival and peak arrival times observed between the two methods can help guide expectations when conducting a field test by providing an approximate arrival "window". In addition, the predicted range of peak concentration values can indicate whether or not the proposed tracer dosage will be adequate for detection through the course of test, particularly if the model is adequatly calibrated to historical operational data. Finally, as previously demonstrated, the full tracer response may have more nuanced character, illustrative of geospatial heterogeneity and dynamic variability within the reservoir system, that the particle tracer methodology can reveal which may be masked by the aqueous component methodology alone. The combination of insights provided by this methodology – particularly when used in conjunction with the conventional aqueous component tracers – can provide a richer picture of a geothermal system's character and can be harnessed by project teams to enhance their overall approach to tracer test design and implementation with very little "cost" (e.g., simulation run time, grid refinement, etc.) on the upfront reservoir engineering evaluation. For the scenarios evaluated in this case study, for example, the additional run time to include four particle tracers (with 1,000 particles per tracer) added less than 10 seconds to the total simulation run time (see Table 2).

Table 2. Comparison of Simulation Run Times for Different Scenarios of Tracer Components

Scenario No.	Unique Particle Tracers	# of Particles Per Tracer	Unique Aqueous Tracers	Run Time (s)
1	4	10,000	4	462
2	0	-	4	322
3	4	10,000	0	289
4	4	1,000	0	171
5	0	-	0	162

5. CONCLUSIONS

In this paper we have presented a new particle tracking system for modelling tracer flow in Volsung and compared it to the traditional approach of using an additional component in the finite volume method. The particle method is easier to use, simulations are faster to run and more complex tracer behaviour, such as thermal or radioactive decay and preferential phase partitioning, can be modelled.

A couple of simple test cases demonstrated that the tracer particle method could reproduce expected tracer arrival times under steady state flow conditions. In these cases, the particle tracking method gave closer results to the theoretical arrival times and did not have as much dispersion as the additional component finite volume method. The tracer particle method was applied to a real-world case by using a full-field model of a producing geothermal field. In this case, 4 tracers were simulated using both the particle method and the additional component approach. Results indicated that the first arrival times in the additional component method were heavily influenced by numerical dispersion and the particle method was able to model more nuanced flow path patterns, such as the bimodal tracer return curve due to the flow across multiple grid layers driven by the interactions between multi-feed zone wells.

This work highlighted the importance of dispersion when modelling tracers in geothermal reservoir simulations. In the real world, hydrodynamic dispersion causes the spreading out of tracer as it flows. In models, numerical dispersion causes the spreading out of tracer as it flows. But hydrodynamic dispersion and numerical dispersion are not the same processes. Hydrodynamic dispersion is a function of the fluid and rock properties while numerical dispersion is dependent on grid block size and the numerical methods used. In science and academia this understanding is well established, but in applied geothermal reservoir modelling it is still common for users to rely on numerical dispersion to reproduce results that were caused by hydrodynamic dispersion. This mismatch in physics can lead to poorly calibrated models and lower confidence in model predictions, such as forecasted thermal breakthrough. The particle method takes steps to overcome this problem by reducing the amount of numerical dispersion, however, it is not a full solution because it does not yet have an explicit model for hydrodynamic dispersion. In future work we will add hydrodynamic dispersion to the particle method in Volsung to improve its ability to model real-world tracer behaviour.

REFERENCES

Arrhenius, S. A.: Über die Dissociationswärme und den Einfluss der Temperatur auf den Dissociationsgrad der Elektrolyte. Z. Phys. Chem. 4 (1889)

Axelsson G., Björnsson G., & Montalvo F.: Quantitative Interpretation of Tracer Test Data. Proceedings World Geothermal Congress (2005)

Baxter, C., Clearwater, J., Franz, P., O'Brien, J., & Williams, B.: Fast-tracking numerical modelling projects using Volsung and Leapfrog Energy. Proceedings New Zealand Geothermal Workshop (2023)

Burnell, J., Sajkowski, L., and Clearwater J.: Modelling Tracer Breakdown Under Geothermal Conditions. Proceedings New Zealand Geothermal Workshop (2021)

Buscarlet, E., Moon, H., Wallis, I., and Jaime Quinao.: Reservoir Tracer Test at the Ngatamariki Geothermal Field, Proceedings New Zealand Geothermal Workshop (2015)

Cinco, F., Franz, P. and Menzies, A.: Testing the Volsung Suite as a Reservoir Simulation software by comparing it with the TOUGH2 Tiwi Model. NGAP Webinar Series: Digital Applications (2020).

Clearwater, J., & Franz, P.: Introducing the Volsung Geothermal Simulator: Features and Applications. Proceedings New Zealand Geothermal Workshop (2019)

Clearwater, J., Güney, A., Yılmaz M. S., Özbek D., Baser A., Saraçoğlu, O. and O'Brien J.: Integrated geothermal asset understanding - The next generation of geothermal simulation. First Break Volume 42 (2024)

Croucher, A., O'Sullivan, M., Kikuchi, T. and Yasuda, Y.: Eulerian–Lagrangian tracer simulation with TOUGH2. Geothermics, Volume 33, Issue 4 (2004)

Croucher, A., Sullivan, J. O., Yeh, A., & Sullivan, M. O.: Benchmarking and experiments with Waiwera, a new geothermal simulator. Proceedings 43rd Workshop on Geothermal Reservoir Engineering, Stanford University, Stanford, CA (2018)

Croucher, A., Sullivan, M. O. & Sullivan, J. O.: Modelling Tracers Using the Waiwera Geothermal Flow Simulator. Proceedings 43rd New Zealand Geothermal Workshop (2021)

Franz, P., Clearwater, J., & Burnell, J. Introducing the Volsung Geothermal Simulator: Benchmarking and Performance. Proceedings New Zealand Geothermal Workshop (2019)

Franz, P., & Clearwater, J.: Volsung: Inverse Modelling and Uncertainty Analysis using PEST. Proceedings New Zealand Geothermal Workshop (2021)

Klausen, Runhild & Rasmussen, Atgeirr & Stephansen, Annette. (2012). Velocity interpolation and streamline tracing on irregular geometries. Computational Geosciences. 16. 261-276. 10.1007/s10596-011-9256-0.

McLean, K., Franz, P., & Clearwater, J.: Swanhild: Numerical Pressure Transient Analysis Using the Volsung Geothermal Reservoir Simulation Package. Proceedings New Zealand Geothermal Workshop (2020)

Oldenburg, C.M. and Pruess, K.: Higher-order differencing for geothermal reservoir simulation. Proc. 22nd Workshop on Geothermal Reservoir Engineering, Stanford University (1997)

Oldenburg, C.M. and Pruess, K.: Simulation of propagating fronts in geothermal reservoirs with the implicit Leonard total variation diminishing scheme. Geothermics 29, 1 – 25 (2000).

Pollock, D.W.: User Guide for MODPATH Version 6—A Particle-Tracking Model for MODFLOW: U.S. Geological Survey Techniques and Methods 6–A41, 58 p. (2012)

Pruess K., Narasimhan T.N.: A practical method for modeling fluid and heat flow in fractured porous media. Society of Petroleum Engineers Journal 25 (1985)

Pruess, K., Oldenburg, C. and Moridis, G.: TOUGH2 user's guide, version 2.0. LBNL-43134, Lawrence Berkeley National Laboratory, Berkeley, California (1999)

Quinao, J., Franz, P. & Clearwater, J.: Well Performance Diagnostics and Forecasting Using the Gudrun Wellbore Simulator – Case Studies From Kawerau, New Zealand. Proceedings New Zealand Geothermal Workshop (2020)

Shook M., & Forsmann H.: Tracer Interpretation Using Temporal Moments on a Spreadsheet. Idaho National Laboratory Geothermal Technologies Program (2005)

Wu, Y. and Forsyth, P.: Efficient Schemes for Reducing Numerical Dispersion in Modeling Multiphase Transport Through Porous and Fractured Media. Proceedings TOUGH Symposium (2006)